

Non-LTE radiative transfer in cool stars.

Theory and applications to the abundance analysis for 24 chemical elements

Maria Bergemann and Thomas Nordlander

Abstract The interpretation of observed spectra of stars in terms of fundamental stellar properties is a key problem in astrophysics. For FGK-type stars, the radiative transfer models are often computed using the assumption of local thermodynamic equilibrium (LTE). Its validity is often questionable and needs to be supported by detailed studies, which build upon the consistent framework of non-LTE. In this review, we outline the theory of non-LTE. The processes causing departures from LTE are introduced qualitatively by their physical interpretation, as well as quantitatively by their impact on the models of stellar spectra and element abundances. We also compile and analyse the most recent results from the literature. In particular, we examine the non-LTE effects for 24 chemical elements for six late-studied FGK-type stars.

1 Introduction

Local thermodynamic equilibrium (LTE) is a common assumption when solving the radiative transfer problem in stellar atmospheres. The reason for adopting LTE is that it tremendously simplifies the calculation of number densities of atoms and molecules. However, the trouble is that the assumption essentially implies that stars do not radiate. Quoting Mihalas and Athay (1973), 'Departures from LTE occur simply because stars have a boundary through which photons escape into space'. In what follows, we will take a short excursus into why this happens and provide a brief overview of the recent developments in the field.

M. Bergemann
Institute of Astronomy, University of Cambridge, Madingley Road, CB3 0HA, Cambridge, UK.
e-mail: mbergema@ast.cam.ac.uk

T. Nordlander
Division of Astronomy and Space Physics, Department of Physics and Astronomy, Uppsala University, Box 516, 75120 Uppsala, Sweden. e-mail: thomas.nordlander@physics.uu.se

We start with reviewing the theoretical foundations of radiative transfer as it happens in reality, i.e. including its impact on the properties of matter in stellar atmospheres. This approach is known as non-local thermodynamic equilibrium (non-LTE). We discuss the non-LTE 'mechanics' and summarise the impact on spectral line formation. Finally, we present a list of non-LTE abundance corrections for the chemical elements, for which detailed statistical equilibrium calculations are available in the literature.

2 The framework and notation

Let us for simplicity take a one-dimensional hydrostatic model of a stellar atmosphere, which is some relation of temperature and gas pressure with depth, and consider the transport of radiation outward.

At each depth point, we then assume that matter particles (ions, atoms, electrons, molecules) are in *local thermodynamic equilibrium* with each other. This equilibrium is established by intra-particle collisions, resulting in the Maxwellian velocity distribution and the Saha-Boltzmann distribution of particles over degrees of excitation and ionisation. Thus the fundamental assumption of LTE is that particle collisions establish the energy distribution of matter. The energy distribution of the radiation field may depart from LTE, $J_\nu \neq B_\nu$, but the influence of non-blackbody radiation field¹ on the energy partitioning of matter is ignored. The local rate of energy generation η_ν depends only on the local thermodynamic properties of the gas, i.e. the local kinetic temperature T_e and local pressure. Therefore the local source function is simply the Planck function B_ν .

However, the physical truth is that photons and matter particles interact in a variety of ways: through photo-excitation and ionisation, radiative recombination, stimulated emission, and other processes. Deep inside the star, typically far below the photosphere, the collision rates are very intense and the photon mean free path l_λ is smaller than the scale over which the physical variables (temperature, pressure) change, so that the radiation field thermalises to the Planck function, $J_\nu \approx B_\nu$. Closer to the stellar surface, l_λ becomes large, larger than the scale height of material. Thus, as photons diffuse outward, their decoupling from matter increases: the radiation field becomes non-local, anisotropic, and strongly non-Planckian. Numerical calculations show that the radiative transition rates driven by the non-local radiation field in the outer atmospheric layers far outweigh collisional transition rates, thus the populations of atomic energy levels differ from the LTE values.

The non-locality arises because of scattering: photons moving through the gas only change their direction in a random way and experience a slight shift in frequency. To account for scattering in the processes of radiative transfer and, correspondingly, establishment of excitation-ionisation equilibrium of an element, the concept of non-LTE was introduced. First, the Saha-Boltzmann equations are re-

¹ A non-blackbody spectral energy distribution is in itself non-LTE.

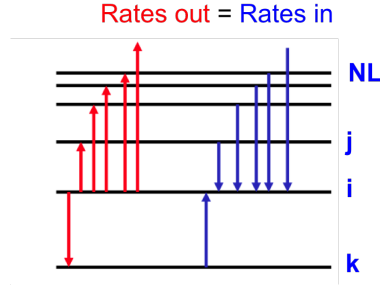


Fig. 1 Illustration of the statistical equilibrium equation for a level i in the model atom; the sum of the rates of all transitions into a level i is balanced by the sum of the rates out.

placed by the rate equations or their time-independent counterpart, statistical equilibrium (SE) or *kinetic equilibrium* equations. For example, an SE equation for a level i , illustrated in Fig. 1, can be written like:

$$n_i \sum_{j \neq i} P_{ij} = \sum_{j \neq i} n_j P_{ji}. \quad (1)$$

Here, $P_{ij} = C_{ij} + R_{ij}$ is the total of collisional and radiative rates (per particle) which establish the equilibrium number of ions excited to the level i . A subscript ij means that a transition from the level i to the level j occurs. This equation must be written for each level i of every ion c in every unit volume of a stellar photosphere, and it describes the microscopic interaction between atoms, electrons and photons.

To close the system of statistical equilibrium equations, the equation of number conservation can be used for a fixed number density of hydrogen:

$$\sum_{i,c} n_{i,c} = \frac{\alpha_{\text{el}}}{\alpha_{\text{H}}} \left(\sum_i n_{i,\text{H}} + n_p \right) \quad (2)$$

where $\alpha_{\text{el}}/\alpha_{\text{H}}$ is the fraction of all atoms and ions of a the element relative to that of hydrogen.

For collisional rates, several theoretical formulae exist, also quantum-mechanical calculations and few experimental data points in the relevant energy regime are available. Collisional rates depend only on the local value of electron temperature and density. For the Maxwellian distribution, the collision-induced transitions from the lower to the upper level in a transition are related to the inverse transitions from the upper to the lower level by the detailed balance principle, i.e. through the Saha-Boltzmann factor $\exp(-E_i/kT)$ and the level statistical weights. The rates of transitions due to inelastic collisions are calculated according to:

$$C_{ij} = n_e \int_{v_0}^{\infty} \sigma_{ij}(v) v f(v) dv \quad (3)$$

where $\sigma_{ij}(\mathbf{v})$ is the electron collision cross-section, $f(\mathbf{v})$ is the Maxwellian velocity distribution, v_0 is the threshold velocity with $mv_0^2/2 = h\nu_0$.

The radiation field enters equation 1 through the radiative rates R_{ij} :

$$R_{ij} = \int_0^\infty \frac{4\pi}{h\nu} \sigma_{ij}(\mathbf{v}) J_\nu d\nu \quad R_{ji} = \int_0^\infty \frac{4\pi}{h\nu} U_{ij} \sigma_{ij}(\mathbf{v}) \left(\frac{2h\nu^3}{c^2} + J_\nu \right) d\nu \quad (4)$$

where $\sigma_{ij}(\mathbf{v})$ is the cross-section of a transition from a state i to a state j , i.e. the monochromatic extinction coefficient per particle in a state i . For bound-bound transitions, $\sigma_{ij}(\mathbf{v}) = \sigma^{\text{line}}(\mathbf{v})$, and for bound-free transitions, $\sigma_{ij}(\mathbf{v}) = \sigma^{\text{cont}}(\mathbf{v})$. The function U_{ij} is expressed as:

$$U_{ij} = \left(\frac{n_i}{n_j} \right)_{LTE} \exp\left(-\frac{h\nu}{kT}\right) \quad (5)$$

where j is a bound level or a continuum energy state. The mean intensities J_ν at all frequencies relevant to the transition $i \rightarrow j$ are derived from the radiative transfer (RT) equation, which can be written in terms of the optical depth τ :

$$d\tau_\nu(z) = -\kappa_\nu dz \quad (6)$$

$$\mu \frac{dI_\nu(\tau_\nu, \mu)}{d\tau_\nu} = I_\nu(\tau_\nu, \mu) - S_\nu(\tau_\nu) \quad (7)$$

For the true (thermal) absorption and emission processes, the source function S_ν is defined by the Planck function. In non-LTE, a part of the local energy emission at a given point is due to the scattering of photons from the surrounding medium. So the source function also depends on the radiation field (see Eq. 13), which is at some frequencies non-local. As a result, we have a coupled system of statistical equilibrium and radiative transfer equations which must be solved simultaneously to give the distribution of particles among excitation levels and ionisation stages.

The solution of the coupled SE and RT equations is non-trivial and beyond the scope of this lecture. The most common method is accelerated lambda iteration (Rybicki and Hummer, 1992).

3 Non-LTE effects

3.1 Statistical equilibrium

To quantify the departures from LTE, it is necessary to explore relationships of the kind $n_{\text{non-LTE}}/n_{\text{LTE}}$, i.e. the number density of a given energy level in an atom or a molecule as computed in non-LTE compared to LTE. This ratio is termed a departure coefficient, b_i . Although there are several definitions, the one given above (Wijbenga

and Zwaan, 1972) is the most common. Under LTE, $b_i = 1$ and the level is said to be 'thermalised', i.e. its occupation number is just as that given by the Saha-Boltzmann statistics. Under non-LTE, if $b_i < 1$, the level is underpopulated, and if $b_i > 1$, the level is overpopulated relative to its value in LTE.

How do these numbers come about? The algorithm is contained in the statistical equilibrium equations, which determine the relative populations of the energy levels to satisfy the given stellar parameters, the gradients of physical variables in the atmosphere², and the intrinsic atomic properties of an atom or molecule under consideration, i.e the structure of electronic configurations and the transition probabilities. To understand this better, we can expand the rates in the SE equation for a level i (Mihalas 1978):

$$\begin{aligned} \text{all transitions to a level } i : & \sum_{j > i} n_j \left(\frac{n_i}{n_j} \right)_{\text{LTE}} (R_{ji} + C_{ji}) + \sum_{k < i} n_k (R_{ki} + C_{ki}) = \\ \text{all transitions from a level } i : & n_i \sum_{k < i} \left(\frac{n_i}{n_j} \right)_{\text{LTE}} (R_{ik} + C_{ik}) + n_i \sum_{j > i} (R_{ij} + C_{ij}) \end{aligned} \quad (8)$$

where j may refer to a bound or a free (ion ground-state or continuum state, and the radiative and collisional rates depend on the mean intensity (eq. 4). The equations contain both the bound-bound and the bound-free terms, so the mean intensity must be integrated either over the line profile or over a large range of energies from the ionisation edge of a given level.

Neglecting all ionisation processes, equation 8 would simplify to:

$$\begin{aligned} \sum_{j > i} n_j \left(\frac{n_i}{n_j} \right)_{\text{LTE}} (A_{ji} + B_{ji}\bar{J} + C_{ji}) + \sum_{k < i} n_k (B_{ki}\bar{J} + C_{ki}) = \\ n_i \sum_{k < i} \left(\frac{n_i}{n_j} \right)_{\text{LTE}} (A_{ik} + B_{ik}\bar{J} + C_{ik}) + n_i \sum_{j > i} (B_{ij}\bar{J} + C_{ij}) \end{aligned} \quad (9)$$

where $\bar{J} = \int \psi_\nu J_\nu d\nu$, A_{ji} and B_{ji} the Einstein coefficients for spontaneous and stimulated de-excitation (emission), C_{ji} the rate of collisional de-excitation; the inverse quantities are represented by the coefficients A_{ik} , B_{ik} and C_{ik} .

Having solved the equations for all levels in a model atom simultaneously with the RT equation at all relevant frequencies, we end up with the *statistical* (or *excitation-ionisation*) *balance*, which gives us the non-LTE values of the atomic number densities n_i ³. The next step is usually the analysis of the individual rates with the aim to understand how exactly the distribution arises, and in particular to identify the leading channel which drives the departures from LTE under the influence of the radiation field.

² Assume that the non-LTE problem is solved for a fixed model atmosphere structure

³ In the literature, the atomic number densities may also be referred to as population numbers

Often, there is no need to analyse each individual rate, as most of them are very small, so in practice the statistical equilibrium is established by one or two dominant channels. These channels are, in essence, sequences of processes, which occur under a certain combination of factors, including the optical depth in a line or continuum, the difference between J_ν and the local Planck function, the relative size of cross-sections for different atomic levels.

These channels are schematically illustrated in Fig. 2, and they include:

- **Photoionisation and photon pumping**

A super-thermal radiation field with mean intensity larger than the Planck function, $J_\nu > B_\nu(T_e)$, leads to over-ionisation (Fig. 2 (a)) and over-excitation (Fig. 2 (d)). The latter process is termed photon pumping. The typical situation is that in a stellar atmosphere the mean intensity in the continuum $J_{\nu,c}$ lies significantly above the local Planck function bluewards of the stellar flux maximum. Thus, over-excitation and over-ionisation affect the neutral atoms (e.g. Mg I, Si I, Fe I), which have ionisation threshold in the blue and UV.

- **Over-recombination**

If the mean intensity falls below the Planck function, $J_\nu < B_\nu(T_e)$, the shortage of ionisations leads to the net over-recombination to the upper levels (Fig. 2 (b)),

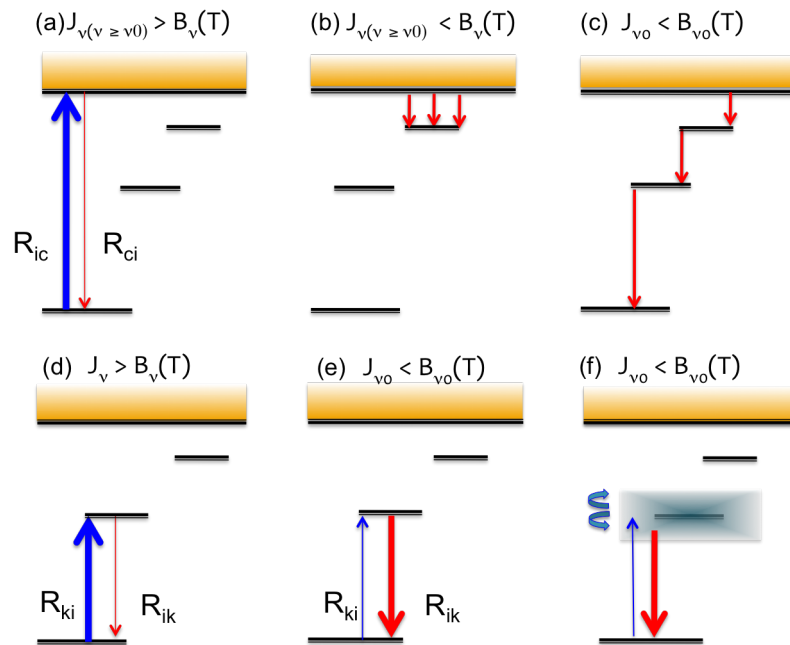


Fig. 2 Illustration of reaction channels for a hypothetical multi-level atom. ν_0 is the central frequency for a spectral line or the frequency of ionisation threshold. See Sec. 3.1

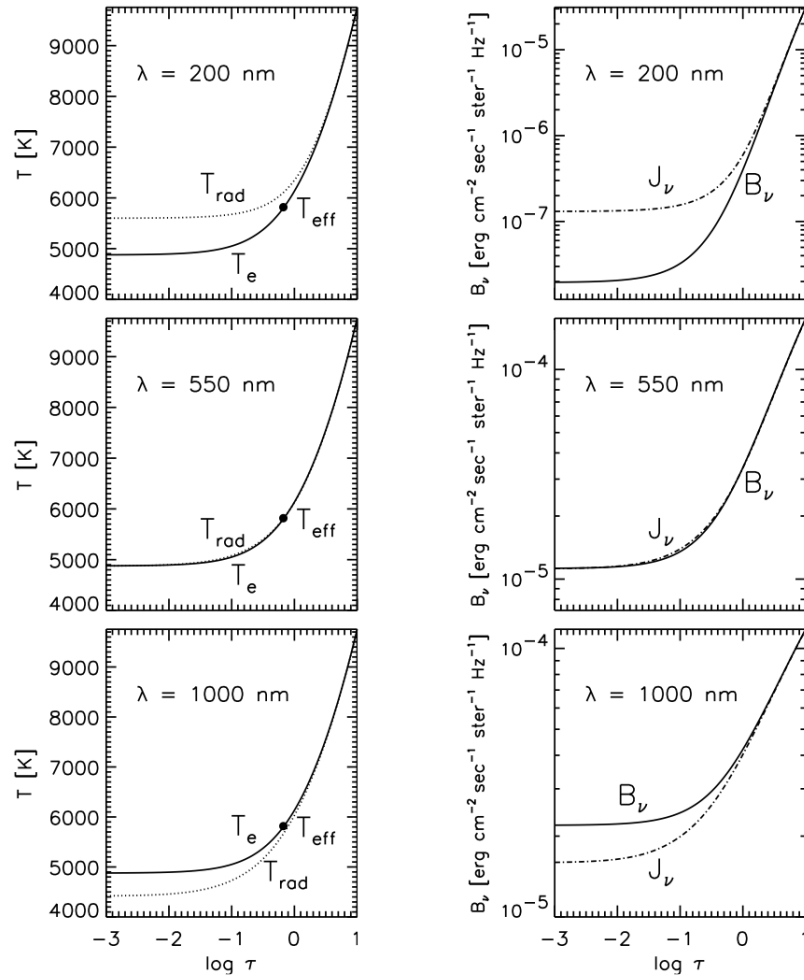


Fig. 3 Left panel: The comparison of radiation temperatures for different wavelengths with the local kinetic temperature in a stellar atmosphere. Right panel: The decoupling of the mean intensity from the Planck function for different wavelengths, as indicated in each sub-plot. Figure courtesy Rob Rutten; <http://www.staff.science.uu.nl/~rutte101>.

as is the case in the infrared (Fig. 3, bottom panel). Over-recombination takes place in the bound-free transitions with the corresponding wavelengths; this is the case for the majority of neutral atoms (Na I, K I, Cr I, Fe I, etc).

- **Photon 'suction'**

For many elements, the diagram of electronic configurations is very regular, with a sequence of high-probability transitions connecting the lowest and the uppermost (Rydberg) levels. This 'ladder' favours photon suction (Fig. 2 (c)), which

represents a successive de-excitation through high-probability transitions to the lower levels. Photon suction is a sequence of spontaneous transitions caused by photon loss, in the atmospheric layers where the line centre optical depth has dropped below unity for every transition involved in the sequence. Such a sequence can include transitions of various frequencies, from UV to IR. Photon suction is balanced by the recombination flow through the bound-free edges in the IR.

- **Photon loss and resonance line scattering**

If the optical depth falls below unity in a line, $\tau_{\nu 0} < 1$, the photons escape without reconversion to thermal energy. This is termed photon loss. In the framework of statistical equilibrium, radiative excitations are in deficit, and spontaneous de-excitations lead to the over-population of the lower level in a transition out of the upper level (Fig. 2 (e), (f)). The effect is particularly important for strong resonance lines (e.g. Na D or Mg b) with very small collisional destruction probability: photon escape in the line itself influences the line source function, causing sub-thermal S_{ν} .

Of course, in most cases all these processes form a sophisticated bundle, which is very difficult to unfold. The non-LTE effects depend upon several factors, including the physical conditions and the atomic structure (ionisation energy, characteristics of the energy levels in the atom, the number of allowed and forbidden transitions, size of cross-sections). However, generally atoms fall into one of the two categories: *photo-ionisation dominated* atoms and *collision-dominated* ions (see Gehren et al, 2001, and references therein):

- **Photo-ionisation-dominated ions**

The main non-LTE driver is over-ionisation. The typical situation is that low-lying energy levels of over-ionising species have very large photo-ionisation cross-sections, and that their ionisation edges are located in the UV, where $J_{\nu} > B_{\nu}(T_e)$. Moreover, the photo-ionisation cross-sections of atoms with complex electronic configurations often have prominent resonances at certain energies which further enhances the radiative rates. For such atoms (e.g., Mg I, Al I, Si I, Ca I, Mn I, Fe I, Co I), the non-LTE departure coefficients are generally below unity, i.e. there is a sub-set of strongly under-populated levels, and this under-population is redistributed over all other levels by collisions or optically thick line transitions. The non-LTE effects usually grow with increasing T_{eff} , and decreasing $[\text{Fe}/\text{H}]$ and $\log g$, due to stronger non-local radiation fields in the UV, lesser efficiency of thermalising collisions, and vanishing line blocking at low metallicity.

- **Collision-dominated ions**

With very small photo-ionisation cross-sections, the statistical equilibrium of collision-dominated ions reflects the interplay between the strong line scattering, over-recombination, and collisional thermalisation. Representative ions with these properties are Na I and K I. We note, however, that this is a general picture in 1D hydrostatic model atmospheres, and may not be valid in the statistical equilibrium calculations with 3D RHD models (see e.g. Lind et al, 2013).

A very detailed discussion of these processes with different thought experiments and toy model atoms, is given in Bruls et al (1992). We also refer the reader to Mihalas and Athay (1973), who provide an excellent physical basis for the qualitative understanding of the overall picture.

3.2 Spectral line formation

Once we know what non-LTE effects dominate the statistical equilibrium of an atom, the behaviour of spectral line profiles is easy to understand. The analysis is aided by the diagrams of level departure coefficients for the levels involved in the transition as a function of some reference optical depth, e.g. the optical depth at 500 nm in the continuum. For the strong lines, it is often helpful to explore the depths of formation of various parts of the line profiles⁴, for example the layers where in the core or in the wing $\tau_V^l = 1$. The emergent intensity within a spectral line is given by the radiative transfer equation:

$$I_V(\tau_V = 0, \mu) = \int_0^\infty S_V(\tau_V) e^{-\tau_V/\mu} d\tau_V/\mu \quad (10)$$

where $\mu = \cos \theta$, for the photons travelling in the direction specified by the angle θ with respect to the normal. The atomic levels populations are contained in the source function S_V and in the optical depth τ_V (eq. 6). The line extinction coefficient (related to τ_V via equation 6), or opacity, is defined by:

$$\kappa_V^l \propto n_i \left(1 - \frac{n_j g_i}{n_i g_j} \right) = b_i \left(1 - \frac{b_j}{b_i} e^{-\frac{h\nu}{kT}} \right) \quad (11)$$

In the Wien's regime ($h\nu > kT$), the expression reduces to:

$$\kappa_V^l \propto b_i \quad (12)$$

When $b_i < 1$, the line opacity is decreased and thus the line formation depth increases. As temperature is higher in the deeper layers, the result is a weakening of the absorption line. The other way around, $b_i > 1$ leads to an increased opacity in the line over an LTE value. The line thus forms in the outer atmospheric layers, where temperatures are lower, which leads to the line strengthening with respect to the continuum.

The line source function can be written as:

⁴ In the literature, one may often find expressions of the following kind: A spectral line is formed 'at a given optical depth'. The usual interpretation of this depth is the location where $\tau_{\lambda,0} = 1$ (at the wavelength of the line core, λ_0) is achieved. Of course, a spectral line forms over an interval of depths. For some strong lines, this range encompasses the whole stellar atmosphere, i.e. several hundred km.

$$S^l = \frac{2h\nu^3}{c^2} \frac{1}{\frac{n_i g_j}{n_j g_i} - 1} = \frac{2h\nu^3}{c^2} \frac{1}{\frac{b_i}{b_j} \left(e^{\frac{h\nu}{kT}} - \frac{b_j}{b_i} \right)} \quad (13)$$

where we make the assumption of complete redistribution in a line profile, which implies that the frequency and direction of an absorbed and emitted photons are not correlated. When $h\nu > kT$ (in the UV and visual spectral range):

$$\frac{S^l}{B_v^l} \approx \frac{b_j}{b_i} \quad (14)$$

A spectral line is weakened when $b_j > b_i$. The situation arises when $S^l > B_v^l$, implying there are more atoms excited to the upper level of a transition j compared to those on the lower level i , than would result under LTE. Hence, there is more emission and less absorption in the line in comparison with the Planck's law. Conversely, the absorption line strengthens when $b_j < b_i$, or $S^l < B_v^l$, as there are not enough atoms on the level j to maintain the same emissivity as in LTE.

Weak lines with small opacity relative to the continuum are formed in the deep atmospheric layers. Their intensity profiles simply reflect the profile of κ_ν . Thus whatever process, i.e over-ionisation or over-excitation, causes smaller line opacity, $b_i < 1$, will result in a weaker absorption line.

Strong lines influence their own radiation field and also the cross-talk between different frequencies within the line is important. The simplest case is that of strong resonance lines, which have a nearly two-level-atom source function. As described above, the surface photon losses cause $J_\nu < B_\nu$ and sub-thermal source function $S^l < B_\nu$, that leads to darker line cores compared to LTE.

In general, there is no simple analytic solution for estimating the effect of b_i inequalities on line profiles. Non-LTE effects may change the equivalent width of a line, but its profile may also be affected, even if the equivalent width is conserved. Thus, departures from LTE may appear in both curve-of-growth and spectrum synthesis methods, with sometimes subtle differences.

4 The impact of non-LTE on elemental abundance analyses

The effects of non-LTE on the abundance determinations in cool stars have been presented in several excellent review articles, perhaps the most up-to-date and comprehensive study is that by Asplund (2005). There is little that can be added to these papers. We thus restrict the discussion to representative groups of chemical elements with similar non-LTE effects, and provide a set of plots, which can be used to gain a qualitative understanding of how the non-LTE abundance corrections vary with stellar parameters. These corrections are shown in Fig. 4 for six well-studied stars with parameters listed in Table 1: the Sun, Procyon, Arcturus, HD 84937, HD 122563,

and HD 140283. The references to the data are given in Table 2 in the Appendix. Figure 5 also shows the results for the individual chemical elements.

Non-LTE abundance correction for a given chemical element, Δ_{El} , is defined as, $\Delta_{\text{El}} = \log A(\text{El})_{\text{non-LTE}} - \log A(\text{El})_{\text{LTE}}$, i.e., it is the logarithmic correction, which has to be applied to an LTE abundance determination A of a specific line to obtain the correct value corresponding to the use of non-LTE line formation.

Several interesting observations can be made based on these plots. For the lines of the photo-ionisation type ions (B I, Mg I, Al I, Si I, Ca I, Sr I, as well as all neutral Fe-peak atoms: Ti I, Cr I, Mn I, Fe I, Co I, Ni I) the non-LTE abundance corrections increase with decreasing metallicity. This tendency simply reflects the fact that the atoms experience a larger degree of over-ionisation and radiative pumping due to stronger $J_V - B_V$ splits in the low-metallicity atmospheres. The spectral lines are weaker in non-LTE compared to LTE, and the non-LTE abundances are correspondingly larger.

For the collision-type minority ions, like Na I and K I, the non-LTE effects on the line formation are mainly due to photon suction and over-recombination. The spectral lines are typically strengthened, with non-LTE abundance corrections in the range from -0.1 to -0.5 dex (Fig. 5). The efficiency of over-recombination, caused by $J_V < B_V$ in the IR, grows with increasing T_{eff} , which is why departures from LTE have the largest effects for warm turn-off stars, like Procyon.

The diagnostic lines of atoms like Li I (671 nm), C I (910, 960 nm), O I (777 nm triplet), Ca II, Sr II, and Ba II, are often stronger in non-LTE. However, the effect depends on stellar parameters, elemental abundance, and the atomic data for a transition (see also Johnson et al, 1974). At higher metallicity, or elemental abundance, the strong lines have sub-thermal source functions due to photon loss through the wings. The non-LTE abundance corrections are negative for C I and O I, as well as for Sr II and Ba II at solar $[\text{Fe}/\text{H}]$. However, the non-LTE effects for Sr II and Ba II drastically change at low-metallicity ($[\text{Fe}/\text{H}] < -2$): the lines tend to be weaker in non-LTE and the abundance corrections grow positive. For Eu II, the positive non-LTE corrections are caused by radiative pumping which weakens the lines, especially in metal-poor stars.

Note that the lines of atoms affected by hyperfine structure (e.g. Mn II, Ba II) should be treated with HFS components also in the non-LTE line formation calculations. This may turn out to be important for higher-metallicity stars.

5 Summary and conclusions

Non-local thermodynamic equilibrium is a framework, which describes consistently the propagation of radiation in a stellar atmosphere and its coupling to matter. LTE

Table 1 Stellar parameters for the selected reference stars. T_{eff} and $\log g$ have been independently determined by fundamental relations, while $[\text{Fe}/\text{H}]$ is the typical literature value.

Star	T_{eff}	$\log g$	$[\text{Fe}/\text{H}]$
Sun	5777	4.44	0.00
Procyon	6545	3.99	-0.05
Arcturus	4247	1.59	-0.52
HD 84937	6275	4.11	-2.00
HD 140283	5720	3.67	-2.50
HD 122563	4578	1.61	-2.74

is the boundary case of non-LTE, the approximation in the limit of infinitely large collision rates.

In this review lecture, the focus is on non-LTE conditions in the atmospheres of cool late-type stars. The impact of non-LTE on stellar parameter and abundance determinations can be gained from detailed theoretical and observational analyses, and these are now available for the most important chemical elements observed in the spectra of cool stars. So far, most studies in the literature focussed on deviations from LTE in the spectral lines of neutral or singly-ionised atoms.

Generally, the results obtained by independent groups and methods are consistent and they can be summarised as follows. There are several well-defined types of non-LTE effects, and consequently several groups of species which behave similarly under the same physical conditions in a stellar atmosphere (i.e. given the same T_{eff} , $\log g$, and $[\text{Fe}/\text{H}]$). The first group is formed by species sensitive to over-ionisation (e.g. Mg I, Si I, Ca I, Fe I), the second group are collision-dominated species (Na I, K I), and the rest are mixed-type ions (e.g. Li I, O I, Ba II), which may show positive or negative non-LTE effects depending upon different factors.

In some cases, the non-LTE abundance corrections vary by an order of magnitude between the groups of elements. In other cases, cancellation may occur such that even the LTE analysis may provide the correct abundance *ratios* of two elements. Such pairs are difficult to establish, although, to first approximation, one may form pairs from elements in the same group, taking into account the excitation potential of the line as well as the elemental abundances. We want to stress, however, that a widely-spread 'rule of thumb' that the lines of the same ionisation stage can be safely modelled in LTE is a misconception.

Generally, any element analysed under the assumption of LTE should be regarded with caution (at least) until careful non-LTE studies have been conducted. Even then, second-order non-LTE effects related to line strengths and excitation potentials may turn out to fundamentally alter the outcome. With these potential pitfalls, we urge the reader to take non-LTE corrections into account whenever possible.

Acknowledgements Fig. 3 has been kindly provided by Rob Rutten.

References

- Asplund M (2005) New Light on Stellar Abundance Analyses: Departures from LTE and Homogeneity. *Annual Review of Astronomy & Astrophysics*43:481–530, DOI 10.1146/annurev.astro.42.053102.134001
- Baumüller D, Gehren T (1997) Aluminium in metal-poor stars. *Astronomy & Astrophysics*325:1088–1098
- Bergemann M (2011) Ionization balance of Ti in the photospheres of the Sun and four late-type stars. *Monthly Notices of the Royal Astronomical Society*413:2184–2198, DOI 10.1111/j.1365-2966.2011.18295.x, 1101.0828
- Bergemann M, Cescutti G (2010) Chromium: NLTE abundances in metal-poor stars and nucleosynthesis in the Galaxy. *Astronomy & Astrophysics*522:A9, DOI 10.1051/0004-6361/201014250, 1006.0243
- Bergemann M, Gehren T (2008) NLTE abundances of Mn in a sample of metal-poor stars. *Astronomy & Astrophysics*492:823–831, DOI 10.1051/0004-6361:200810098, 0811.0681
- Bergemann M, Pickering JC, Gehren T (2010) NLTE analysis of CoI/CoII lines in spectra of cool stars with new laboratory hyperfine splitting constants. *Monthly Notices of the Royal Astronomical Society*401:1334–1346, DOI 10.1111/j.1365-2966.2009.15736.x, 0909.2178
- Bergemann M, Hansen CJ, Bautista M, Ruchti G (2012a) NLTE analysis of Sr lines in spectra of late-type stars with new R-matrix atomic data. *Astronomy & Astrophysics*546:A90, DOI 10.1051/0004-6361/201219406, 1207.2451
- Bergemann M, Lind K, Collet R, Magic Z, Asplund M (2012b) Non-LTE line formation of Fe in late-type stars - I. Standard stars with 1D and μ 3D_z model atmospheres. *Monthly Notices of the Royal Astronomical Society*427:27–49, DOI 10.1111/j.1365-2966.2012.21687.x, 1207.2455
- Bergemann M, Kudritzki RP, Würl M, Plez B, Davies B, Gazak Z (2013) Red Supergiant Stars as Cosmic Abundance Probes. II. NLTE Effects in J-band Silicon Lines. *The Astrophysical Journal*764:115, DOI 10.1088/0004-637X/764/2/115, 1212.2649
- Bruls JHMJ, Rutten RJ, Shchukina NG (1992) The formation of helioseismology lines. I - NLTE effects in alkali spectra. *Astronomy & Astrophysics*265:237–256
- Caffau E, Maiorca E, Bonifacio P, Faraggiana R, Steffen M, Ludwig HG, Kamp I, Busso M (2009) The solar photospheric nitrogen abundance. Analysis of atomic transitions with 3D and 1D model atmospheres. *Astronomy & Astrophysics*498:877–884, DOI 10.1051/0004-6361/200810859, 0903.3406
- Fabbian D, Asplund M, Carlsson M, Kiselman D (2006) The non-LTE line formation of neutral carbon in late-type stars. *Astronomy & Astrophysics*458:899–914, DOI 10.1051/0004-6361:20065763, astro-ph/0608284
- Gehren T, Butler K, Mashonkina L, Reetz J, Shi J (2001) Kinetic equilibrium of iron in the atmospheres of cool dwarf stars. I. The solar strong line spectrum. *Astronomy & Astrophysics*366:981–1002, DOI 10.1051/0004-6361:20000287

- Gehren T, Shi JR, Zhang HW, Zhao G, Korn AJ (2006) Na, Mg and Al abundances as a population discriminant for nearby metal-poor stars. *Astronomy & Astrophysics*451:1065–1079, DOI 10.1051/0004-6361:20054434
- Johnson HR, Milkey RW, Ramsey LW (1974) Formation of the Luminosity-Sensitive 0 I Multiplet at 7774 Å. *The Astrophysical Journal*187:147–150, DOI 10.1086/152600
- Kiselman D, Carlsson M (1996) The NLTE formation of neutral-boron lines in cool stars. *Astronomy & Astrophysics*311:680–689, astro-ph/9601144
- Kunc JA, Soon WH (1991) Analytical ionization cross sections for atomic collisions. *The Journal of Chemical Physics*95:5738–5751, DOI 10.1063/1.461622
- Lind K, Asplund M, Barklem PS (2009) Departures from LTE for neutral Li in late-type stars. *Astronomy & Astrophysics*503:541–544, DOI 10.1051/0004-6361/200912221, 0906.0899
- Lind K, Asplund M, Barklem PS, Belyaev AK (2011) Non-LTE calculations for neutral Na in late-type stars using improved atomic data. *Astronomy & Astrophysics*528:A103, DOI 10.1051/0004-6361/201016095, 1102.2160
- Lind K, Bergemann M, Asplund M (2012) Non-LTE line formation of Fe in late-type stars - II. 1D spectroscopic stellar parameters. *Monthly Notices of the Royal Astronomical Society*427:50–60, DOI 10.1111/j.1365-2966.2012.21686.x, 1207.2454
- Lind K, Melendez J, Asplund M, Collet R, Magic Z (2013) The lithium isotopic ratio in very metal-poor stars. *Astronomy & Astrophysics*554:A96, DOI 10.1051/0004-6361/201321406, 1305.6564
- Mashonkina L, Gehren T, Bikmaev I (1999) Barium abundances in cool dwarf stars as a constraint to s- and r-process nucleosynthesis. *Astronomy & Astrophysics*343:519–530
- Mashonkina L, Korn AJ, Przybilla N (2007) A non-LTE study of neutral and singly-ionized calcium in late-type stars. *Astronomy & Astrophysics*461:261–275, DOI 10.1051/0004-6361:20065999, astro-ph/0609527
- Mashonkina L, Zhao G, Gehren T, Aoki W, Bergemann M, Noguchi K, Shi JR, Takada-Hidai M, Zhang HW (2008) Non-LTE line formation for heavy elements in four very metal-poor stars. *Astronomy & Astrophysics*478:529–541, DOI 10.1051/0004-6361:20078060, 0711.4454
- Mashonkina L, Ryabtsev A, Frebel A (2012) Non-LTE effects on the lead and thorium abundance determinations for cool stars. *Astronomy & Astrophysics*540:A98, DOI 10.1051/0004-6361/201218790, 1202.2630
- Mihalas D, Athay RG (1973) The Effects of Departures from LTE in Stellar Spectra. *Annual Review of Astronomy & Astrophysics*11:187, DOI 10.1146/annurev.aa.11.090173.001155
- Reetz JK (1998) Sauerstoff in kühlen Sternen und die chemische Entwicklung der Galaxis
- Rybicki GB, Hummer DG (1992) An accelerated lambda iteration method for multilevel radiative transfer. II - Overlapping transitions with full continuum. *Astronomy & Astrophysics*262:209–215

- Sitnova TM, Mashonkina LI, Ryabchikova TA (2013) Influence of departures from LTE on oxygen abundance determination in the atmospheres of A-K stars. *Astronomy Letters* 39:126–140, DOI 10.1134/S1063773713020084
- Takeda Y, Zhao G, Chen YQ, Qiu HM, Takada-Hidai M (2002) On the Abundance of Potassium in Metal-Poor Stars. *Publications of the ASJ*54:275–284, astro-ph/0110165
- Takeda Y, Hashimoto O, Taguchi H, Yoshioka K, Takada-Hidai M, Saito Y, Honda S (2005) Non-LTE Line-Formation and Abundances of Sulfur and Zinc in F, G, and K Stars. *Publications of the ASJ*57:751–768, astro-ph/0509239
- Wijbenga JW, Zwaan C (1972) Empirical NLTE Analyses of Solar Spectral Lines. I: A Method and Some Applications to Earlier Analyses. *Solar Physics*23:265–286, DOI 10.1007/BF00148089
- Würl M (2012) NLTE analysis of silicon lines in solar-type stars and red supergiants
- Zhang HW, Gehren T, Zhao G (2008) A non-local thermodynamic equilibrium study of scandium in the Sun. *Astronomy & Astrophysics*481:489–497, DOI 10.1051/0004-6361:20078910
- Zhao G, Butler K, Gehren T (1998) Non-LTE analysis of neutral magnesium in the solar atmosphere. *Astronomy & Astrophysics*333:219–230

Table 2 References to NLTE studies of late-type stars in the literature, which were used to create Figs. 4 and 5.

Ion	S_H	Reference	Spectral lines [nm]
Light elements			
B I	x^a	Kiselman and Carlsson (1996)	250
Li I	QM ^b	Lind et al (2009) ^c	670.7
C I	0	Fabbian et al (2006)	909.5
N I	1/3	Caffau et al (2009)	12 lines, $744 \leq \lambda \leq 1054$
O I	0	Reetz (1998)	777.1–777.5
O I	1	Sitnova et al (2013)	615.8, 777.1–777.5, 844.7
Intermediate elements			
Na I	QM ^b	Lind et al (2011) ^c	568.8, 589.5, 615.4, 819.4
Mg I	x^d	Zhao et al (1998)	13 lines, $457 \leq \lambda \leq 892$
Mg I	0.05	Gehren et al (2006)	7 lines, $457 \leq \lambda \leq 571$
Mg I	0.1	Mashonkina et al (2008)	6 lines, $457 \leq \lambda \leq 571$
Al I	0.4 ^e	Baumüller and Gehren (1997)	396.2, 669.7
Al I	0.002	Gehren et al (2006); Mashonkina et al (2008)	396.2
Si I	1	Bergemann et al (2013) ^f ; Würfl (2012)	9–10 lines, $390 \leq \lambda \leq 723$
S I	1	Takeda et al (2005)	8 lines, $869 \leq \lambda \leq 1046$
K I	0.001	Takeda et al (2002)	769.9
Ca I	0.1	Mashonkina et al (2007, 2008)	422.6, 442.5, 526.1, 534.9, 616.2
Sc I	0.1	Zhang et al (2008)	567.2
Sc II	0.1	Zhang et al (2008)	552.6
Ti I	0.05	Bergemann (2011)	453.4, 498.1, 502.2, 843.5
Fe-group elements			
Cr I	0	Bergemann and Cescutti (2010)	425.4, 520.6, 540.9
Mn I	0.05	Bergemann and Gehren (2008)	475.4, 467.1, 601.6, 874.0
Fe I	1	Bergemann et al (2012b); Lind et al (2012) ^c	492.0, 499.4, 521.6, 524.2, 606.5, 625.2, 643.0
Co I	0.05	Bergemann et al (2010)	350.1, 411.0, 412.1
Zn I	1	Takeda et al (2005)	472.2, 481.1, 636.2
Neutron-capture elements			
Sr I	0	Bergemann et al (2012a) ^c	460.7
Sr II	0	Bergemann et al (2012a) ^c	407.7, 421.5, 1004, 1033, 1091
Pb I	0.1	Mashonkina et al (2012)	405.7
Th II	0.1	Mashonkina et al (2012)	401.9, 408.6
Eu II	0	Mashonkina et al (2008, 2012)	413.0
Ba II	0	Mashonkina et al (1999, 2008)	455.4, 585.3, 649.6 1&3)

^a H I collision rates for ionisation from Kunc and Soon (1991); no b-b collisions included in the model atom.

^b Based on quantum mechanical calculations of hydrogen collision rates

^c Results were extracted using www.inspect-stars.net

^d S_H set as exponentially dependent on upper excitation energy

^e But $S_H = 0.002$ for levels where $n > 7$, affecting IR lines.

^f Corrections were computed specifically for this work

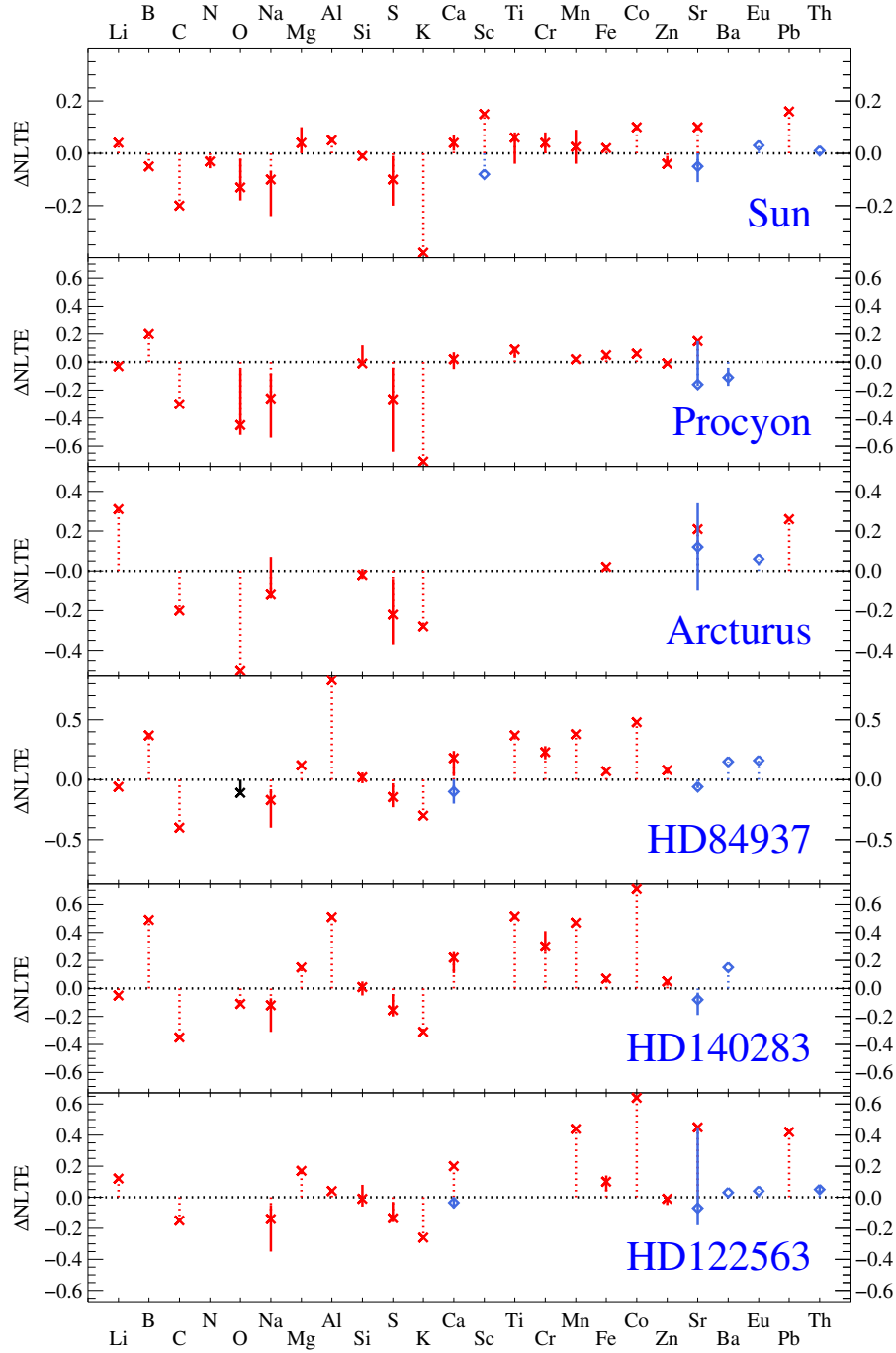


Fig. 4 Non-LTE effects on 24 elements for six representative, well-studied stars. Non-LTE (NLTE) effects are given as abundance corrections $\Delta\text{NLTE} = A(X)_{\text{NLTE}} - A(X)_{\text{LTE}}$. Red crosses and blue diamonds show results obtained from the lines of neutral and ionised atoms, respectively. Solid, vertical lines indicate min–max ranges of the corrections. The O I non-LTE correction for Arcturus is the limiting value taken from Sitnova et al (2013, Fig. 5). For HD 84937 we adopt the same value as for HD 140283, since Reetz (1998) found the same values for stars with similar parameters.

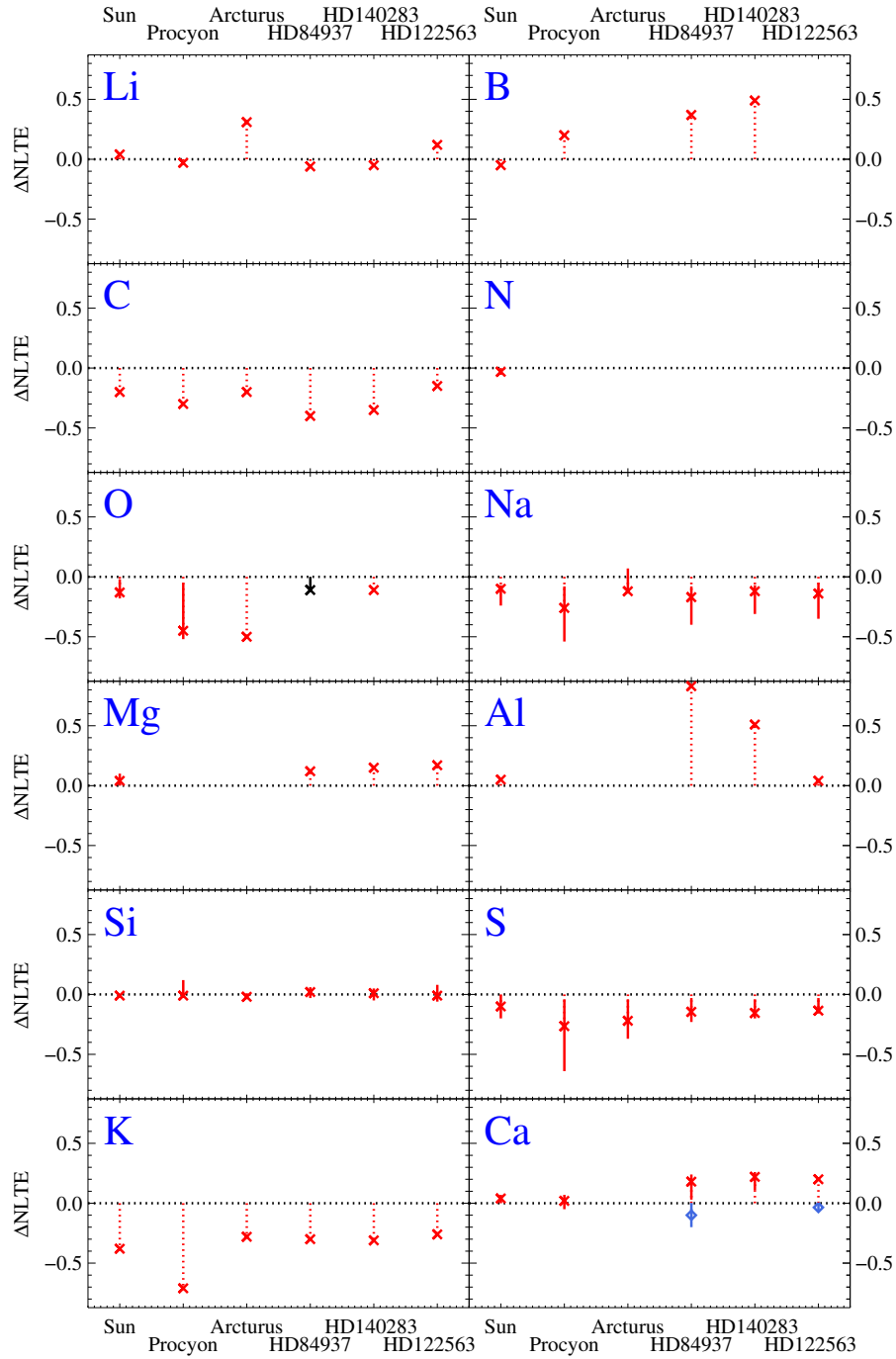


Fig. 5 As Fig. 4, but element-by-element.

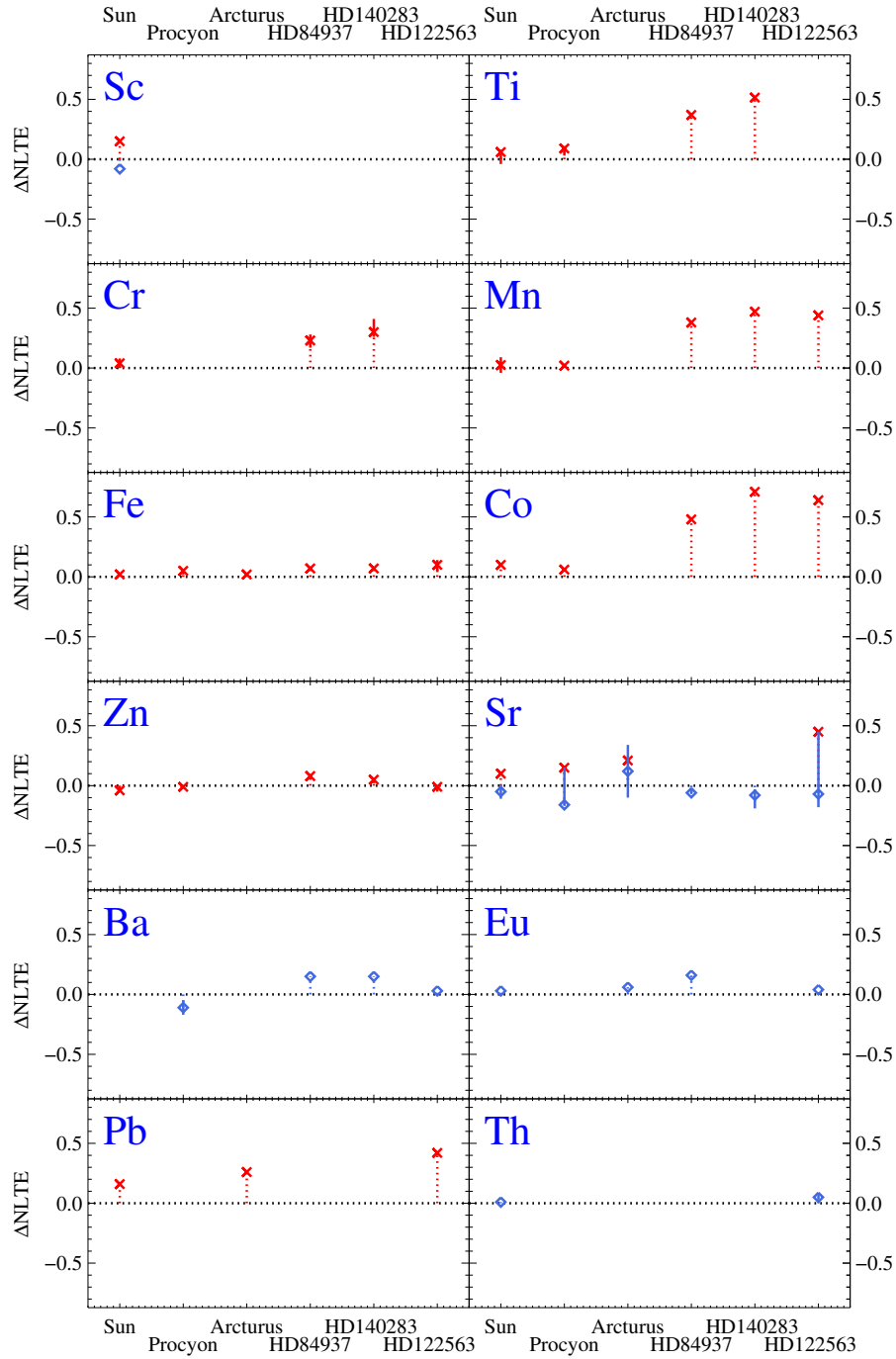


Fig. 5 continued.